Detection and Processing of Bistatically Reflected GPS Signals From Low Earth Orbit for the Purpose of Ocean Remote Sensing

Scott Gleason, Stephen Hodgart, Yiping Sun, Christine Gommenginger, Stephen Mackin, Mounir Adjrad, and Martin Unwin

***Abstract*—We will show that ocean-reflected signals from the global positioning system (GPS) navigation satellite constellation can be detected from a low-earth orbiting satellite and that these signals show rough correlation with independent measurements of the sea winds. We will present waveforms of ocean-reflected GPS signals that have been detected using the experiment onboard the United Kingdom's Disaster Monitoring Constellation satellite and describe the processing methods used to obtain their delay and Doppler power distributions. The GPS bistatic radar experiment has made several raw data collections, and reflected GPS signals have been found on all attempts. The down linked data from an experiment has undergone extensive processing, and ocean-scattered signals have been mapped across a wide range of delay and Doppler space revealing characteristics which are known to be related to geophysical parameters such as surface roughness and wind speed. Here we will discuss the effects of integration time, reflection incidence angle and examine several delay-Doppler signal maps. The signals detected have been found to be in general agreement with an existing model (based on geometric optics) and with limited independent measurements of sea winds; a brief comparison is presented here. These results demonstrate that the concept of using bistatically reflected global navigation satellite systems signals from low earth orbit is a viable means of ocean remote sensing.**

***Index Terms*—Bistatic radar, global navigation satellite systems (GNSS), global positioning system (GPS), delay-Doppler mapping, oceanography, QuikSCAT, reflectometry, satellite remote sensing.**

I. Introduction

When electromagnetic radiation scatters off the ocean surface, the scattering process changes the characteristics of the propagating signal in a way that is dependent on the reflecting surface. These changes contain information on the sea surface waves and indirectly on the near-surface meteorological conditions. Most radar-based ocean remote sensing is founded on this general principle. Notably, this concept was quantitatively demonstrated over a half a century ago by Cox and Munk using photographs of the sun glitter off the ocean surface [1].

Since then there have been numerous advancements and demonstrations of this process to remotely sense various ocean phenomenon. However, most of the systems in use to date are actively transmitting radar pulses and then detecting the received power of the backscattered radiation. An alternative concept of ocean remote sensing was proposed by scientists at the European Space Agency in 1993 [2],[1] and later the same principle was suggested as a tool to sense sea roughness [3]. The concept proposes that a similar technique to that of traditional radar remote sensing can be applied to bistatically reflected signals transmitted from global navigation satellites, such as those of global positioning systems (GPS) and in the future those of the Galileo navigation constellation. Although in a broad sense the techniques of bistatic and traditional radar remote sensing are similar, the scattering processes involved for each could prove to be significantly different. For example, the Bragg scattering that often dominates in traditional radar has been given limited attention so far in the case of forward scattering.

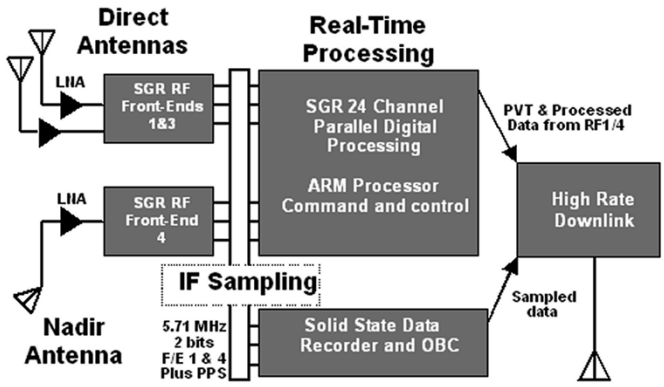

Fig. 1. Experiment configuration on the UK-DMC satellite. The experiment includes a total of three antennas: two space pointing that are used for normal GPS navigation operations and a third downward pointing, higher gain, left-hand circularly polarized (LHCP) antenna for targeting signals scattered off the earth's surface. It is possible to process the data both in real time using the onboard capability as well as occasionally downloading intermediate frequency (IF) raw sampled data for more intensive postprocessing on the ground.

Manuscript received August 8, 2004; revised January 17, 2005.

S. Gleason is with Surrey Satellite Technology, Ltd., University of Surrey, GU2 7XH, Guildford, U.K. and also with the Surrey Space Centre, University of Surrey, Guildford, GU2 7XH, U.K. (e-mail: s.gleason@sstl.co.uk)

S. Hodgart, S. Mackin, and M. Adjrad are with the Surrey Space Centre, University of Surrey, Guildford, GU2 7XH, U.K.

Y. Sun is with Fujitsu Laboratories of Europe, Ltd., Hayes, UB4 8FE, U.K.

C. Gommenginger is with the Ocean Circulation and Climate Division, National Oceanography Centre, Southampton, SO14 3ZH, U.K.

M. Unwin is with Surrey Satellite Technology, Ltd., University of Surrey, Guildford, GU2 7XH, U.K.

Digital Object Identifier 10.1109/TGRS.2005.845643

[1]See also U.S. Patent 5,546,087 (Aug. 13, 1996).

TABLE I
SUMMARY OF INITIAL RAW DATA COLLECTIONS. APPROXIMATELY 20 s OF SAMPLED DATA WERE DOWN LINKED FROM A SINGLE SPACE-FACING ANTENNA AND THE DOWNWARD POINTING ANTENNA ON EACH OF THE ABOVE DATES. IN EACH CASE, ALL SPECULAR REFLECTION POINTS IN THE 3-dB FOOTPRINT OF THE ANTENNA WERE FOUND. CONCERNING START AND END LOCATIONS, DUE TO OCCASIONAL DROPS ON THE TELEMETRY DATA BUS, THE LOCATIONS FOR SOME COLLECTIONS WERE ADJUSTED TO THE FIRST AND LAST AVAILABLE TELEMETRY PACKET

No.	Start Date/Time (UTC)	Start Location (WGS84)	End Location (WGS84)	Signals Found	Model Estimated Wind Speed	Processed Signal to Noise	3dB Doppler Bandwidth
1	12th March 2004, 9 : 00 : 43	Lat 29.9348N Lon 158.2833W Alt 686962 m	Lat 28.7877N Lon 158.5793W Alt 686953 m	PRN 27	3.0 m/s	5.3	2800 Hz
2	23rd March 2004, 08 : 05 : 53	Lat 50.1179S Lon 159.1032W Alt 712882 m	Lat 51.1217S Lon 159.5364W Alt 713250 m	PRN 28	2.5 m/s	4.0	2300 Hz
3	6th April 2004, 08 : 32 : 33	Lat 15.5077S Lon 158.1031W Alt 698791 m	Lat 16.5947S Lon 158.3466W Alt 699061 m	PRN 28	15.5 m/s	1.9	4200 Hz
4	21st May 2004, 08 : 46 : 42	Lat 21.5358N Lon 155.9058W Alt 682394 m	Lat 20.4447N Lon 156.1600W Alt 682182 m	PRN 29 PRN 26	7.1 m/s 8.9 m/s	2.3 2.5	3300 Hz 3500 Hz
5	24th May 2004, 09 : 02 : 52	Lat 16.2777N Lon 160.7757W Alt 680624 m	Lat 15.1849N Lon 161.0194W Alt 680508 m	PRN 29 PRN 26	13.2 m/s 14.0 m/s	1.2 1.6	$>$ 6000 Hz 4600 Hz
6	3rd June 2004, 08 : 50 : 32	Lat 0.6617N Lon 159.9394W Alt 679945 m	Lat 0.5543S Lon 160.1965W Alt 680158 m	PRN 29 PRN 26	14.1 m/s 9.1 m/s	1.6 1.9	5600 Hz $>$ 6000 Hz

This measurement technique is original in several ways, primarily in that it uses a passive receiver for bistatically reflected signals, generated by external sources. This results in greatly reducing the amount of instrumentation required onboard the detection vehicle (i.e., a transmitter is not required), making the practicalities of a spaceborne demonstration of the concept realizable [4]. Second, the unique range coded modulation of the GPS signals, allows for the mapping of received power as a function of both time- delay and Doppler frequency across the ocean surface.

Since the first demonstrated space-based detection of an ocean-reflected GPS signal [5] the research community has been searching for a dedicated experiment to more definitively prove that this concept was viable at spacecraft altitudes. The datasets that have been collected from the GPS bistatic remote sensing experiment onboard the United Kingdom's Disaster Monitoring Constellation (UK-DMC) satellite serves this purpose. This paper will present selected time delay and Doppler profiles of the ocean-reflected signals found in the downlinked data and make initial attempts to link these waveforms to sea winds. Additionally, details of the data processing techniques used to produce the waveforms shown will be described in moderate depth. The comparisons of the detected signals with *in situ* and remotely sensed sea measurements is the focus of ongoing research [6], only initial results will be presented here.

II. EXPERIMENT DESCRIPTION

A. Instrumentation

A GPS bistatic remote sensing experiment comprising of a GPS receiver, solid state data recorder and antennas was added to the UK-DMC satellite as a secondary payload and launched in October of 2003. The UK-DMC is one of a small constellation of 700 km altitude polar-orbiting satellites intended to image disaster areas and provide images to relief agencies around the globe. A block diagram of the experiment hardware is shown in Fig. 1.

The satellites of the Disaster Monitoring Constellation normally use two of the GPS antennas for rapid position determination. For this experiment a third, higher gain, downward pointing, left-hand circularly polarized antenna was added for the purposes of detecting ocean-reflected GPS signals. This antenna has a peak gain of 11.8 dBiC and is off pointing 10° "behind" the satellite, which is opposite to the normal satellite velocity vector. The relatively low gain provides a useful benefit, a noticeably larger ocean footprint than could be achieved with a higher gain antenna. For the UK-DMC antenna the along track and cross track 3-dB beamwidth angles are 28° and 67°, respectively, projecting a large area of ocean coverage often encompassing multiple reflections. Additionally, an interface to a solid state data recorder was added to perform raw data logging of the down-converted signals from a single upward-looking navigation antenna as well as for the downward pointing antenna.

The GPS receiver used is Surrey Satellite Technology Limited's Space GPS Receiver,[2] based on the Zarlink (formerly GEC Plessey) chipset [7]. The software has been previously upgraded to perform Delay-Doppler mapping of reflected GPS signals as described in [8], in a similar manner to that of the Parallel Delay Mapping Receiver described in [9], but with the added feature of being able to map the signal as a function of Doppler frequency as well. The experiment is designed with the dual capabilities of processing data in real-time as well

[2]See http://www.sstl.co.uk/datasheets/Subsys_SGR1020_HQ.pdf.

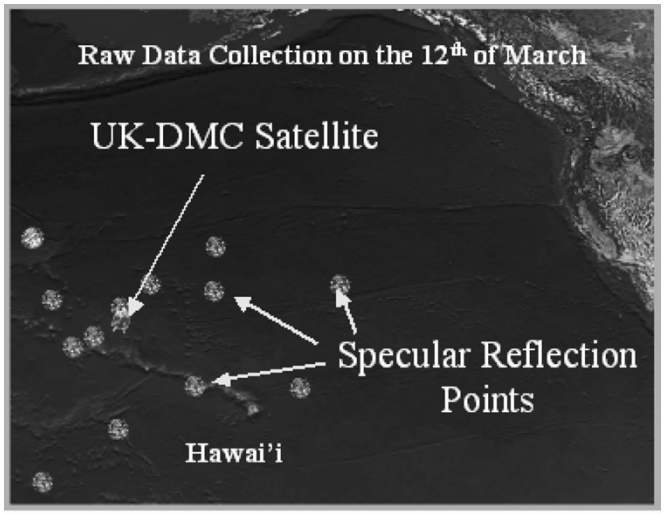

Fig. 2. Location of the first raw data collection on March 12, 2004. The satellite is traveling south with the white patches surrounding it representing predicted specular reflection points on the oceans surface. The specular reflection point just to the north of the satellite is that of GPS satellite number 27, the signal of which was subsequently detected using ground processing.

as logging and downloading raw sampled data from the GPS receiver for more intensive postprocessing on the ground. The signals shown below were all detected using ground processing on down linked raw datasets as sampled by the onboard data recorder. Following, the repeated analysis of these down linked datasets can be used to enhance the real-time signal mapping capability onboard the satellite and eventually perform ocean remote sensing in near real time.

B. Operations and Data Collection

As of the first week of June 2004 the raw data collections summarized in Table I were executed and down linked from the UK-DMC satellite. A detailed representation of the time and place of the first raw data collection, performed on March 12, 2004, is shown in Fig. 2. Data collections are chosen based on several criteria. Initially it must be determined that a specular reflection of one or more GPS satellites lie in the 3-dB footprint of the antenna on the ocean surface. Additionally, the presence of independent measurements at the time and location of the data collection is considered. Independent measurements could come from stationary buoys or even intersections with other ocean remote sensing satellites such as QuikSCAT or JASON.

When a desirable data collection time is found using the ground utilities, a request is made to the satellite operations team and an attempt is made to schedule the data capture on the satellite. In the later phases of this experiment it is hoped to collect data over ice and land surfaces in addition to oceans in an attempt to detect signals off different and often irregular surfaces. For a more detailed description of the bistatic remote sensing experiment and the methods of scheduling data collection opportunities, see [4] or for a demonstration of the real-time processing capabilities [8].

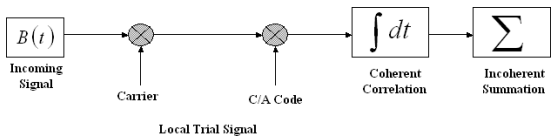

Fig. 3. Diagram of correlation process performed on the received signal, including mixing with local signals, coherent correlation, and noncoherent summations. Trial values of Doppler and delay (ω_T and τ_T) are varied to generate delay Doppler maps.

III. Signal Processing Overview

A. Coherent Versus Noncoherent Integration

In the following analysis several modifications have been made to the traditional GPS signal correlation process to suit our application. The largest of these simplifications lies in how the carrier phase is treated in the analysis, including the quasirandom phase shifts introduced by the GPS navigation data message.

As with most GPS signal processing, we begin by performing a coherent correlation over 1 ms of data. By coherent we mean that the signal is processed using both its in-phase and quadrature signals components separately, with the possibility of computing a carrier phase angle based on these two values. For the application of ocean remote sensing the detected signals are expected to be largely incoherent, for signals scattering from the ocean surface undergo a mixing of phases due to the interaction with the sea surface. Additionally, any phase information is lost when the signal magnitude is computed by squaring and adding the in-phase and quadrature signal components. Following, in our processing the phase components can be initially neglected.

A series of 1-ms coherent correlations are then accumulated, as shown in Fig. 3, resulting in a mapping of the correlation power magnitude across a range of delays and Doppler frequency shifts. This accumulation of consecutive milliseconds is the noncoherent summation (or looks) referred to below. It is possible to integrate coherently over longer or shorter periods of time and then accumulate the correlation powers in a similar manner. Varying the coherent integration interval to arrive at an optimal value will be investigated as part of our ongoing research.

Initial results seem to indicate that the widening of the Doppler bandwidth that occurs when using shorter coherent integration periods obscures significant information in the delay-Doppler map. However, this needs to be weighed against the possible increased signal amplitude that could result from using shorter than 1-ms coherent integration times, as was demonstrated in [5]. Varying the integration time, affects the length of time needed to achieve the required looks at the surface, and ultimately, the measurement resolution. For longer coherent integration times, such as 5 ms for example, a total of 1 s of data is needed to take 200 looks to extract the signal shape, the same amount of time that normally produced 1000 looks using the nominal 1-ms coherent integration. During this time the specular point on the ocean surface is continually in motion. To achieve 1000 looks at 5-ms coherent integration

would require 5 s of data, over which time the specular reflection point will move tens of kilometers and we are no longer strictly looking at the same point.

B. Brief Discussion of the Signal Search Process

To recover reflected GPS signals, the sampled data must be correlated with a locally generated replica with the appropriate code phase and Doppler frequency shift repeatedly over a range of delays and frequencies (see [10] or [11] or any other basic text on global positioning systems for a more detailed discussion of GPS signals). The selection of centers for the search frequencies and delays during this process can be approached in several ways including:

1) Estimate the frequency and time delay using available navigation information over a limited range of frequencies and delays until a combination of values that produces a successful correlation is found.
2) Use fast Fourier transforms to perform correlations at all delays for a given frequency in one step. This process is not described here but more information can be found in [12].
3) Methodically search over all possible time delays and a complete or partial range of possible frequencies offsets.

Whatever method is chosen, it is necessary to accumulate correlations over several milliseconds to discover the true shape of the scattered signal, which can then be used to invert sea information. As the signal is accumulated over time, while taking into account the changing dynamics, the overall signal correlation power can be determined as a function of delay and frequency. All searches involve correlating locally generated replicas with the raw sampled data at the output of the GPS receiver front-end, followed by changing the delay and frequency in small steps and repeating, thus eventually producing the one dimensional delay waveforms (where the Doppler is set constant and the delay is varied) to a full mapping of the signal in time and frequency space where both dimensions are searched.

Because, as mentioned above, the signal will be noncoherently summed over several 1-ms intervals, the effects of the system dynamics on the summation process needs to be considered. For the results shown here the maximum incoherent summation interval used was 1 s. However, a general consideration can be made for an incoherent summation interval of 1 s. In this case we would have to consider the first and second derivative terms of both the received code delay and the frequency terms making the analysis significantly more complicated. From our experience, we found that when the summation interval is limited to 1 s, the only term that has a noticeable effect on the correlation result is the velocity component of the code delay. Our processing neglects the higher order derivative terms relating to delay and all dynamics related frequency terms over the incoherent integration interval. It has been observed that the relative (i.e., the change in the center frequency between the 1st and 1000th incoherent summation of the reflected signal) center frequency changes on the order of several ten of hertz over 1 s. This may result in some "blurring" between Doppler bins but is otherwise negligible.

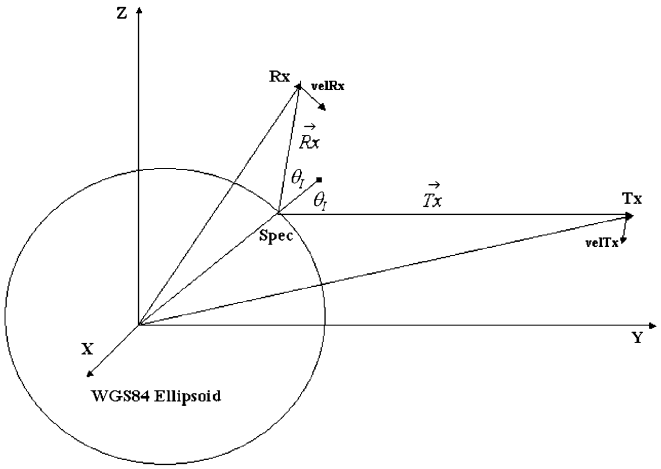

Fig. 4. Reflection geometry. Rx and Tx represent the receiving spacecraft and the transmitting GPS satellite, respectively. The point on the earth's surface where a specular reflection occurs will satisfy Snell's law, where the incident and reflected angles are equal (θ_I). The specular point is assumed to lie on the WGS-84 Ellipsoid.

For the purposes of signal detection we are correlating the signal with both the locally generated in-phase and quadrature components to extract the magnitude only. Coherent phase correlation is needed more for other applications such as absolute ranging in the case of performing sea height estimation, where the phases of the C/A code (several meters) and that of the L1 carrier (centimeters) can both be used to determine an absolute range and hence an ocean height estimate. This application has been explored in depth elsewhere [13], [14].

Another important consideration of the coherent integration interval is the extent to which longer coherent integrations can be used to eliminate cross-correlation between power in adjacent Doppler bins. The degree to which this can be accomplished will determine the unique area on the oceans surface corresponding to a delay-Doppler correlation and hence the achievable surface resolution.

In essence we must perform a signal search in the frequency domain and in the time domain. Position and velocity information provided during the normal GPS receiver operation is used to narrow the ranges of these searches considerably.

The practical implementation involves integrating outward from the specular point along iso-range lines of constant delay (as described in [9]) while holding the frequency constant over the entire integration period. Subsequently, the trial frequency is changed and the process repeated. The maximum signal peak will be achieved using an initial frequency estimate at the point of specular reflection and then gradually scanning over the entire possible range of iso-Doppler lines where it is believed scattered signal power is present. This was what was done in generating the delay-Doppler maps presented in Section V.

The ability to integrate coherently for longer than 1 ms is something that on most GPS receivers is needed only in a limited sense, indoor GPS for example. In the case of signals scattered from the ocean surface a noncoherent summation technique is required. More importantly the end results are different, where in a traditional GPS data processing configuration the output

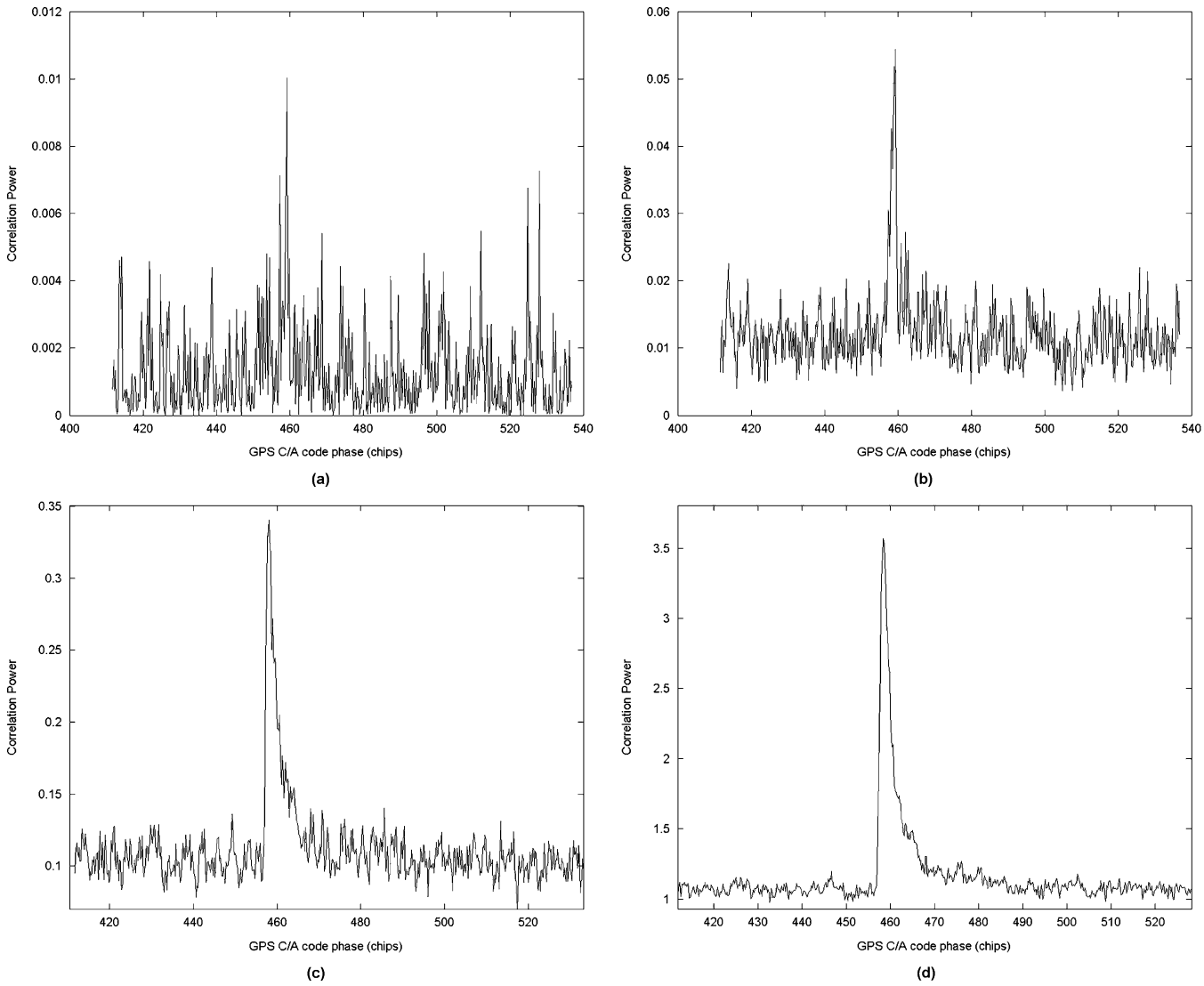

Fig. 5. (Left to right) Signal found in March 12 dataset, for GPS satellite PRN 28, using noncoherent integration times of (a) 1 ms, (b) 10 ms, (c) 100 ms, and (d) 1 s.

is a pseudorange measurement, phase measurement, and a decoded navigation data stream; in the case of bistatic GNSS remote sensing we are interested in the time and frequency correlation shapes. For these shapes are in theory related to the sea surface [15], [16]. Again, Fig. 3 illustrates the basic steps performed to generate individual points in the delay Doppler map.

C. Effects of Incoherent Integrations on Processed Signal-to-Noise Level

The noncoherent accumulation process, acts to both recover the signal shape from the effects of speckle noise as well as to increase the postprocessed SNR level. The signal gradually becomes visible as longer and longer summation times are used (see Figs. 4 and 5). At each millisecond of integration, the contribution of a single look at the surface is accumulated. This is consistent with how signal waveforms are generated when detected from an incoherently scattering surface, such as in traditional radar remote sensing applications and outlined in [17] and [18]. A given number of looks are required to distinguish any signal through the speckle noise due to the incoherent scattering. However, an additional effect of the integration technique used is to raise the processed SNR level, thus slowly bringing the weakest signals above the noise floor. The more looks you take at a given area the more average scattering power appears through the noise. To demonstrate this, we can represent the output of the correlation process in the receiver for two cases, the first where there is no signal present and the output is only correlated noise

$$P_n' = N_n \tag{1}$$

and a second case where the correlated power is a combination of noise and ocean-reflected signal such that

$$P_n'' = X_n + N_n \tag{2}$$

where X represents the scattered signal power and N that of the uncorrelated noise. We can now represent the noncoherent

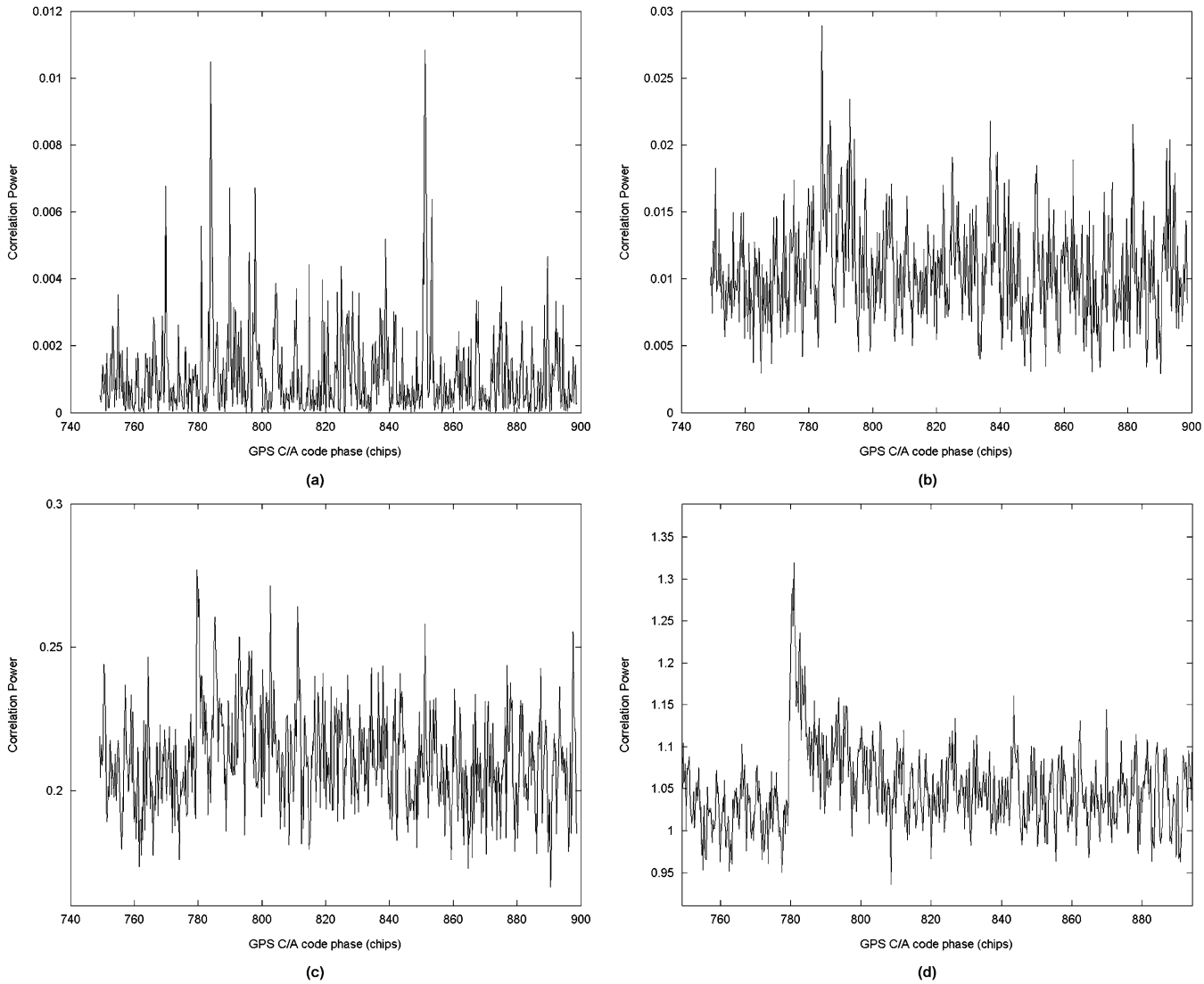

Fig. 6. Signal found in the May 24 dataset, for GPS satellite PRN 29, using noncoherent integration times of (a) 1 ms, (b) 10 ms, (c) 200 ms, and (d) 1 s.

averaging process as the summation of consecutive correlations M, such that

$$\overline{P'_M} = \frac{1}{M}(P'_1 + P'_2 + \cdots P'_M) \tag{3}$$

$$\overline{P''_M} = \frac{1}{M}(P''_1 + P''_2 + \cdots P''_M). \tag{4}$$

It is then useful to look for a positive difference between the two

$$\overline{P_{\text{diff}}} = \overline{P''_M} - \overline{P'_M}. \tag{5}$$

Using the derivation as presented by Elachi [18] as a guide and applying standard statistics procedure, the expected variance of the mean is reduced by a factor of M from the variance of the actual measurements

$$\text{Var}(\overline{P'_M}) = \frac{\text{Var}(P')}{M} \tag{6}$$

$$\text{Var}(\overline{P''_M}) = \frac{\text{Var}(P'')}{M} \tag{7}$$

and the resulting output SNR can then be shown as

$$\text{SNR}_0 = \frac{\overline{P_{\text{diff}}}^2}{\text{Var}(\overline{P''_M}) + \text{Var}(\overline{P'_M})} \tag{8}$$

or

$$\text{SNR}_0 = \frac{M\overline{P_{\text{diff}}}^2}{\text{Var}(P'') + \text{Var}(P')}. \tag{9}$$

As the signal is averaged over a long enough duration the signal shape gradually appears above the noise. This was demonstrated during prelaunch testing and shown to be reliable for notably weak signals [19]. As more and more samples are integrated onto the composite signal, the variance of the noise gradually reduces, thus revealing the signal correlation shape. In theory, this implies that all signals, no matter how weak, can be "detected" using a long enough integration period. However, practicalities will prohibit this and these limits need to be explored.

A practical demonstration of the signal processing procedure is important to move out of the purely theoretical domain and into the realm of real systems. The following demonstrations

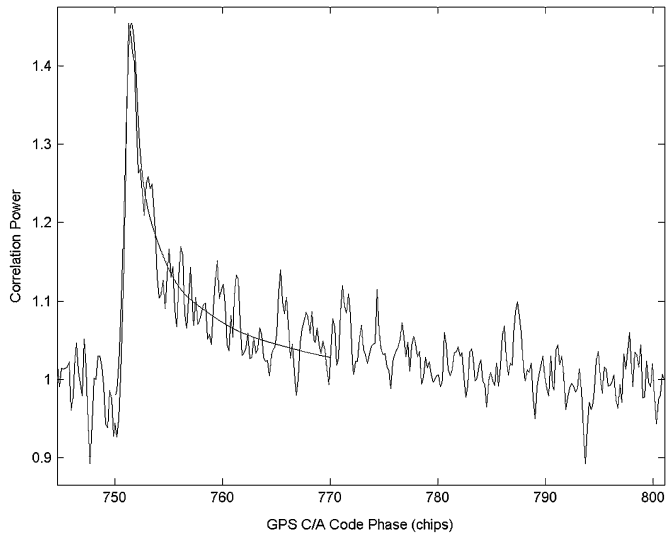

Fig. 7. Ocean-reflected signal in the June 3 dataset from GPS PRN 29 at approximately 7° incidence after 1 s of integration. The signal is shown together with a model-generated waveform using a wind speed of 13 m/s. At various seconds within the data the optimal fit of the model waveform could vary considerable. In this case between 9 m/s and the maximum tested wind speed of 16 m/s.

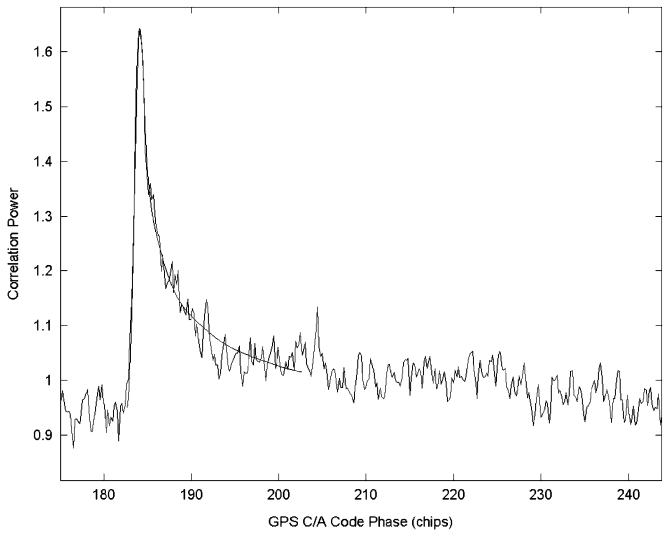

Fig. 8. Ocean-reflected signal in the June 3 dataset from GPS PRN 26 at approximately 17° incidence after 1 s of integration. The signal is shown together with a model-generated waveform using a wind speed of 9 m/s. At various seconds within the data, the optimal fit of the model waveform could vary considerable. In this case between 5 and 12 m/s wind speeds over the range of 6 s.

of time- and frequency-domain waveform mapping provide the foundation building blocks upon which more advanced techniques can be built. Next, a model will be implemented that will allow us to predict what the outputs of the above signal processing might yield in the unique case of a bistatically scattered GPS signal.

IV. Modeling the Expected Signals

We have used outputs from our implementation of the widely used Zavorotny/Voronovich ocean scattering model [15] combined with sea condition inputs based on the Elfouhaily wave spectrum [16] to generate signals for comparison purposes. The general geometry of a bistatic GPS reflection is shown in Fig. 4.

The above discussion focused on general signal detection for a general GPS range coded signal. In the case of bistatically scattered GPS radiation, the signal undergoes a scattering process at the earth's surface before being processed at the GPS receiver. This process needs to be modeled for the purposes of predicting the signal shapes we will measure.

Others have undertaken the challenge of modeling an ocean-reflected GPS signal with some success. The existing methods all derive more or less from the bistatic radar equation that has been used for decades by scientists in analysing the scattering of electromagnetic waves from various surfaces [20]. Our formulation for the reflected signal waveform is based on the work of Zavorotny and Voronovich

$$P_M = \frac{P_1 \lambda^2}{(4\pi)^3} \iint_S \frac{\Re(S) G_{Tx}(S) \sigma^0(S) G_{Rx}(S)}{R_{Rx}(S)^2 R_{Tx}(S)^2} \times \Lambda^2(\tau, \tau_T) \mathrm{sinc}^2(f_T, f_D)\, dS \quad (10)$$

where

P_1	transmit power of GPS satellite;
G_{Tx}	directional transmitter antenna gain;
G_{Rx}	directional receiver antenna gain;
R_{Tx}	path length from transmitter to point on surface S;
R_{Rx}	path length from receiver to point on surface S;
λ	signal wavelength, $\sim$19 cm for the case of GPS L1;
σ^0	dimensionless, normalized scattering coefficient;
$\Re$	polarization-dependent Fresnel reflection coefficient;
$\Lambda(\tau_T, \tau)$	GPS correlation (triangle) function;
$\sin c^2(f_T, f_D)$	attenuation due to Doppler misalignment;
S	arbitrary surface, centered at the point of specular reflection;
dS	significantly small differential area within S where it can be reasonably assumed that the scattering cross section remains constant.

The above formulation is consistent with the standard representations in the existing literature. At this point it suffices to say that the foundations of our model for the scattering of GPS signals off the ocean surface is based on the bistatic radar equation and agrees with the previous work on the subject. However, as described in some existing texts [17], the received signal consists of both a coherent and scattered component. This representation, based on geometric optics and excluding all Bragg effects, assumes only incoherent scatter from the ocean surface, represented by σ^0.

For our initial requirements this formulation is adequate. However, it should be kept in mind that models in general are often only of limited use given the extremely complicated task of modeling the sea surface and its relation to metrological parameters, particularly wind. It may prove more useful to concentrate on empirical methods for sensing various ocean parameters, taking as an example current scatterometry methods

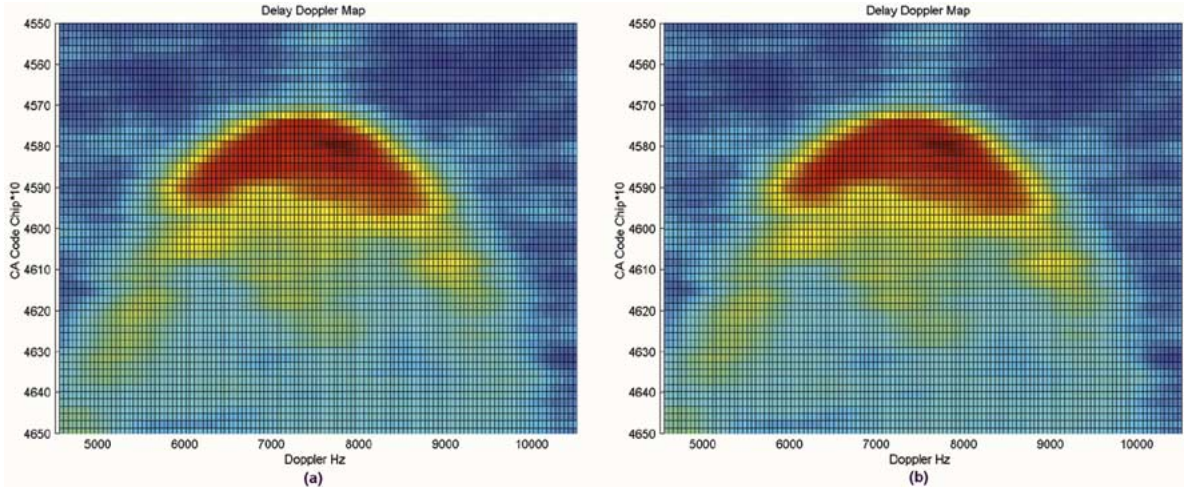

Fig. 9. Delay-Doppler maps of the ocean-reflected signals found in the March 12 dataset. (a) Signal in the 12th second of data after 200 ms of 1-ms summation. (b) The 13th second, also using 200 ms of 1-ms summation. The movement of the signal, between 3 and 4 C/A chips, or just over a kilometer is visible.

for sensing winds. Given the early stage of this technology, we should be open to both sides of the modeling and/or empirical debate, and eventually be able to compare, or merge, one with the other in constructive ways, as was done for the case of scatterometry in [21].

V. Ocean-Reflected Signals

A. Ocean-Reflected Signals Found Using the Methods Described Above

Figs. 5–10 show ocean-reflected signals found in the raw data using the above processing methods. There are several reasons why we believe that the signals detected and found consistently throughout the raw sets have been scattered off the ocean surface.

The most significant reason is the fact that the simulated model waveforms show good agreement with those of the detected signals; the process of fitting the model waveforms with the detected signals is described in more detail in Section VI. The signal shape is also in agreement with the signal detected by the Jet Propulsion Laboratory from the Space Shuttle [5] and with other aircraft-based signal detections [22], [23].

Below is a summary of additional evidence for reflected signals and against other external effects that could disguise themselves as the waveforms we are seeing.

1) The delay and Doppler frequency centers can be predicted to within a constant offset and are distinctly different from the direct (GPS transmitter to receiver) signals detected at the same time.
2) The fact that the signals have been consistently detected across the entire 20 s of data rule out the possibility of cross-correlations from another GPS satellite (due to the change of frequencies involved).
3) Local multipath would not be expected to exhibit itself with the shapes nor the delays and Doppler offsets observed.
4) The delay-Doppler maps of the detected signals indicate that the signal is present over a large area of time and frequency space. This would be expected for incoherently scattered power from the oceans surface and not representative of a direct signal of any sort.

Having said that, the final proof will lie in the eventual connection of the signal waveforms with an ocean observable, such as the sea surface winds, which has already been generally observed, and will be the focus of much future research.

B. Effects of Noncoherent Integration

The effects of noncoherent integration described previously can be demonstrated using any one of the reflected signals detected in the existing datasets. We have chosen a relatively strong signal (that of GPS PRN 28 detected on March 12, Fig. 5) to contrast with a weak signal detected under what are believed to be rough seas (that of GPS PRN 29 on May 24, Fig. 6).

In the case of the stronger signal of March 12, the signal is partially visible after only 1 ms of integration. However, it can be seen that several additional looks need to be taken to extract the real signal shape. The signal shape is distinguishable after both 10 and 100 ms of summation and additional smoothing was achieved by accumulating up to 1 s.

In contrast, the signal found on May 24, shows a much noisier signal, which could only be seen above the noise floor after 200 ms of summation. After 10 ms of summation the shadow of the signal can be made out upon close inspection, but with respect to the noise floor across the entire range of delays it could not be said for sure if this was signal or just a noise effect. It was necessary to perform 200 1-ms summations before the signal could be seen distinctly from spurious noise peaks across the entire range of possible delays. Subsequently, after 1 s of 1-ms summations the signal reveals itself in the expected form. For this example, the longer period of noncoherent summation is increasing the processed SRN as described in (9).

C. Effect of Incidence Angle on the Signal Correlation Shape

For the last three raw datasets collected, two separate ocean-reflected signals were found throughout the entire 20-s data collection interval, in each case those of GPS satellites PRN 29 and PRN 26. This allows us to make a comparison of the effect of

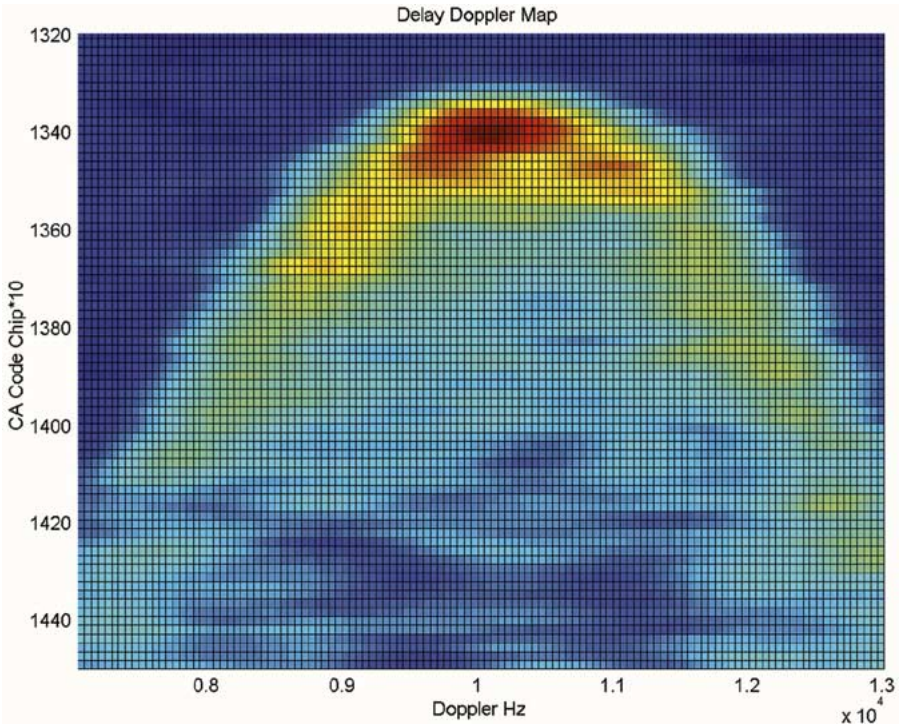

Fig. 10. Delay-Doppler map of the ocean-reflected signal of GPS satellite PRN 26, found in the May 21 dataset. A coherent correlation time of 1 ms and an incoherent summation time of 1 s were used to calculate the correlation power shown in each delay-Doppler bin of this map.

incidence angle on the overall shape of the waveforms, since the locations of the two specular reflection points resulted in different incidence angles (or inversely, grazing angles) at the receiver.

The effect on the signal due to geometry must be eliminated before any estimate can be made concerning the ocean surface. These include several terms of (10), including path delays, antenna gain patterns, and reflection coefficients, all approximated to the best of our knowledge for these examples. The transmitting and receiving antenna patterns were modeled, and the exact locations of the GPS transmitter and the UK-DMC satellite were known as determined from the 1-Hz navigation solution output as part of normal operation of the GPS receiver. Complicating the analysis is the fact that for two specular reflection points separated by a considerable distance, it cannot be assumed that the ocean conditions are sufficiently correlated, where significant wind variations are possible over the vast areas under consideration.

Shown in Figs. 7 and 8 are a pair of detected signals found in a dataset that contained two specular reflection points within the antenna 3-dB footprint, in this case on June 3, 2004. The horizontal axis is GPS C/A code chips, which correspond roughly to 293 m or 1 μs of delay, and the vertical axis is correlation magnitude.

The signals were found using the above-described techniques with an summation interval of 1 s and are shown together with an approximate batch least squares fitting of the simulated model delay waveform as described above.

D. Delay-Doppler Signal Maps

To appreciate the true importance of an ocean-scattered signal it is necessary to generate a delay-Doppler map showing the correlated signal power over a range of frequency bins and time delays. The delay-Doppler Map is best visualized using a three-dimensional rotated representation, with Doppler frequency shown on the horizontal axis and delay on the vertical with signal strength represented as a color scale. Figs. 9 and 10 show maps generated for signals found in March 12 and May 21 datasets, respectively. Fig. 9 is a Delay-Doppler Map of the very first and strongest signal found to date at two consecutive seconds in time. The movement of the signal from 1 s to the next is noticeable in the changing delay on the vertical axis between the two images. It also becomes apparent that the signal spread varies between seconds although the general shape remains the same. This variation needs to be studied carefully in order to optimize the best way to fit the model functions and invert ocean statistics. A consideration of the complete delay-Doppler map, as demonstrated in [24] may turn out to be the most robust, albeit a computationally intensive, method. For strong signals such as this one, where the processed SNR reached as high as 7 dB at times, the process should be easier than for weaker signals such as those found in May 21 data and shown in Fig. 10.

The final signal image is that of the relatively weak GPS PRN 26 reflection after performing 1 s of noncoherent summations over a complete range of delay and Doppler bins. The incident angle of the specular reflection point was approximately 21° from the subsatellite point. At a larger incidence the effects of the antenna beam pattern and geometry will have a greater influence on the signal spread acting in conjunction with the dominant factor contributing to spreading, the sea waves. The larger spread of the signal in delay and Doppler is visible when compared to the March 12 signal. Efforts are underway to determine the sea conditions at the times and places of the different

data collections as part of the process to develop inversion algorithms, described briefly in the next section.

These delay-Doppler maps are similar to what was expected from our signal modeling and that have been shown in other simulations [25]. The distinct horseshoe shape expected is clearly evident. These plots were generated by finely stepping across delay and Doppler space until the majority of the signal power was detected. For the purposes of inverting sea state parameters it is possible to divide the surface into small patches of limited resolution and make a measurement using only the power reflected off that patch. This will be the subject of future research, including the determination as to what resolution and to what accuracy the maps shown below can be broken apart and analyzed.

An interesting feature in these plots is a clearly noticeable asymmetry that could have applications in the determination of wind and wave direction. This utilization of the signal anisotropy has been previously presented using the analysis of signals found during aircraft campaigns [26].

VI. Estimation Techniques

A. Model Fitting to the Detected Waveforms

Initially, model waveforms were generated from (10) using trial wind speeds input into the wave spectrum of [16] to obtain the directional mean square slopes of the surface waves. The resultant suite of waveforms was then fitted by minimizing the cost function shown below in (11). In essence we are varying the wind speed across a wide range of values, and together with the reflection geometry, finding a suitable match for the observed waveform

$$\varepsilon = \sum_{k}^{k_l} [A_R P_M(U_{10}, k - \tau_M) - P_R(k)]^2 \qquad (11)$$

where

- τ_M delay of the peak of the model waveform;
- A_R magnitude of the model waveform, scaled to fit the actual signal level;
- U_{10} wind speed 10 m above the ocean surface, as input into the Elfouhaily wave spectrum;
- k_l number of aligned samples between the detected and model waveforms;
- P_R correlation power delay response, the detected signal waveform;
- P_M model predicted correlation power delay response.

The model-generated delay waveforms and those of the signals found in the raw datasets were matched using a batch least squares method involving five parameters; noise floor, peak power (A_R), delay (τ_M), wind speed (U_{10}), and length of chips (k_l). The noise floor is calculated by taking the mean of a limited number of measurements at delays before the start of the signal. The peak power is determined to be the maximum point of the signal waveform. When the noise floor and the peak power have been determined the model waveform is then scaled using these minimum and maximum values respectively. Next, the cost function is optimized with respect to delay. As the model waveform delay is adjusted over values of τ_M the cost function minimizes for a given delay offset, this offset is then set constant for all wind speeds. The least squares cost function ε is then minimized for waveforms generated under different wind speeds U_{10}, ranging from 2–16 m/s in steps of 1 m/s. The model waveforms were compared over a limited set of samples k_l, for the least squares procedure, lengths of 10, 12.5, 15, 17.5, and 20 chips were all tested. This procedure was executed for a minimum of three different signals (all computed using 1 s of noncoherent summation) and the average was determined to be the best fit for the detected signal, and hence the model wind speed estimate shown in Table I.

TABLE II
Comparison With Independent Sea Measurements. The QuikSCAT Data Used in Each Case Were the "Best Available," Considering the Collocation With the UK-DMC Data Collection Time and Specular Reflection Point Location. In All Three Cases, 0.25° Gridded QuikSCAT Products Were Used. The Temporal Separation Between QuikSCAT and UK-DMC Measurements on the May 21, May 24, and June 3 Were, Respectively, +3 h 13 min (QS Lagging), +2 h 57 min (QS Lagging), and 3 h 10 min (QS Lagging)

Date	PRN	Wind Estimate ECMWF	Wind Estimate QuikSCAT	Model Estimated Wind Speed
21st May 2004	29	6.3 m/s	7.7 - 8.0 m/s	7.1 m/s
	26	5.3 m/s	5.9 - 6.8 m/s	8.9 m/s
24th May 2004	29	6.2 m/s	10.8 - 11.8 m/s	13.2 m/s
	26	5.3 m/s	7.3 - 8.0 m/s	14.0 m/s
3rd June 2004	29	6.7 m/s	6.7 - 6.9 m/s	14.1 m/s
	26	6.5 m/s	6.4 - 6.6 m/s	9.7 m/s

This is not an attempt to validate the model in rigorous detail, for there are too many unknowns in the system and several approximations were deemed necessary. For example, the antenna bore sight direction was not corrected for spacecraft attitude, the antenna gain pattern was only roughly modeled and the wind direction was always arbitrary but equal for all the model waveforms. Regardless, we have managed to show how the signals detected vary with respect to geometry and sea conditions and how the existing models could be used to account for these observed changes. This is the most convincing proof that the signals being detected have been scattered from the ocean surface.

B. Preliminary Ocean Remote Sensing

We have chosen to highlight the data collections that occurred where *in situ* measurements were considered to be trustworthy, using satellite measurements from the QuikSCAT scatterometer. Independent measurements of sea winds existed from QuikSCAT that covered the exact locations over the data collections for May 21 and 24, as well as for June 3. There was also reasonable consistency between the independent measurements taken both before and after the time of data collection, indicating that the sea was probably not varying greatly over the hours in question. As an additional check, the outputs of the European Centre for Medium Range Weather Forecasting (ECMWF) model were used to predict the sea winds over the same area in an attempt to provide a higher level of confidence. Table II shows the wind estimates from the ECMWF weather model, the best available QuikSCAT measurements, and a wind estimate obtained from the Zavorontny/Voronovich model waveform described above for the last three data collections.

From the table it can be seen that the sea seemed to be roughest on May 24, there is agreement between the signals, models and the independent sources as well as in the noisy appearance and low SNR that indicate that the ocean was probably quite rough. The estimates on the other two days indicate that, although not as windy as on May 24, there was still a significant presence of wind induced waves on May 21 and June 3, possibly slightly higher winds on June 3. Unfortunately, the strongest signals were those of March 12 and 23, where the relative SNRs reached as high as 7 and 5 dB, respectively. No reference data was available to draw conclusions from and make comparisons with the reflected signals found on these dates.

Upon detailed inspection the QuikSCAT data for May 21 reveals that the seas may well have been calmer at the location of satellite 26's specular reflection as compared with the location of satellite 29's specular reflection. We are in effect taking two measurements using sea-reflected signals at different places in parallel. We can in theory trace those two points across the ocean surface for as long as the specular reflection points remain visible. The signal model was not able to distinguish this possible difference, but it is possible that the sea conditions had changed slightly or more likely that the noise on the trailing edge of the signal had an exaggerated influence on the least squares model fitting, especially at increased wind speeds.

The primary difficulties encountered so far have been the lack of accurate independent measurements at the exact times and locations of the specular reflection points and, as mentioned, the large amount of noise on some of the signals, even after 1 s of averaging. The former made any attempt to determine the accuracy of the wind speed detection capabilities problematic and the latter making the fitting of the model waveforms difficult. Both of these issues can be overcome with time as more data are collected and the system subtleties become fully understood and compensated for when necessary. This experiment was intended to bring issues like this to the surface so that future missions can adjust and optimize their designs.

C. Discussion of Future Estimation Strategies

A primary focus of this paper was to present some of the ocean-reflected signals found and describe the methods used to find them. However, it has always been our intention to use these signals to remotely sense the earth's environment, not only that of the ocean but possibly over land [27] and ice surfaces [28] as well. The methods to do this have been advanced to some degree by the data processed during aircraft campaigns. It has been shown that it is possible to extract sea wind information by analysing both the trailing edge of the detected signal as well as by fitting the entire waveform [22]. We intend to concentrate initially on the fitting of the entire waveform to model predictions as described above to invert surface statistics. Although this is the most mature method in some regards, other methods could also prove valuable. For example, it has been demonstrated that by using information contained in the Doppler spread of the waveform, statistics related to the surface slopes can be inverted [29], and very approximate estimates of the Doppler half power bandwidths have been provided as a crude test of this proposal. It has also been suggested that there is a sea state dependence on the ratio of right-hand to left-hand circularly polarized radiation present [30] in the detected signals. Unfortunately, the polarization of the antenna on the UK-DMC is left-hand circular only. Future experiments and missions should have this capability for it could result in a relatively quick inversion that could be performed with a minimum of processing.

It should be kept in mind that the requirements for a useful scientific instrument differ from those of a system intended to, for example, improve maritime- safety for the general public. It is thought that for applications that do not require high levels of accuracy or spatial precision, the relative SNR may be of use in sensing the presence of dangerous seas. Although not applicable to systems demanding high accuracy, such a method could be of use in averting accidents at sea. By developing a warning system that could enable ship captains to avoid potentially dangerous seas it would be possible to prevent disasters such as that which occurred in 2002 off the coast of Africa.

To realize such a system several obstacles need to be overcome. In normal scatterometry applications, using the absolute returned signal power to sense the ocean is augmented by an array of instruments that estimate the various atmospheric attenuations present and make corrections. There is substantial evidence that the longer wavelength L-band signals transmitted by the GPS constellation will be less affected by the atmospheric attenuations that complicate the higher frequency instruments [31]. For the experiment configuration on the UK-DMC, matters are complicated by the fact that the absolute signal level is adjusted by an automatic gain control; hence, the power levels of the received signals are relative. However, the effects of the automatic gain control can be estimated and current work is examining the link between sea surface winds/roughness and the processed power levels.

An important part of the model inversion assessment is to gather suitable validation data from independent measurement sources. Currently, such an exercise is underway using primarily the National Oceanic and Atmospheric Administration buoy network and overpasses of both the QuikSCAT and JASON satellites. These sources provide information on wind speed, significant wave height and ocean mean square slopes that can be used in refining the model fit to the reflected GPS signals. Over the lifetime- of the UK-DMC experiment it will be possible to build up a large database of such measurements for validation under a wide range of ocean conditions.

VII. Conclusion

Considering only the existing datasets at the time- of writing; of the nine possible ocean-reflected signals contained within the 3-dB limits of the antenna bean pattern, all nine have been detected. The signal shapes exhibit the general characteristics that have been predicted by existing models and detected on previous aircraft and spaceborne experiments. The initial results shown here are intended to convey primarily that GPS signals scattered from the ocean surface are detectable on a repeatable basis from low earth orbit, and that these signals vary in general accordance with the best knowledge of the sea conditions at the times and places of the measurements.

It has been shown that by using a direct method of noncoherent summations of 1-ms coherent correlations, signals can be reliably detected. We have shown here that the bistatically scattered GPS signals are detectable using available hardware from a low earth orbiting spacecraft. There were numerous doubts that the ocean-scattered signals would be too weak to be detected above the background noise given the relatively low gain of the antenna and high altitude of the experiment configuration. This has proven not to be the case and ocean-scattered signals are being detected on a regular basis. This is good news for all involved, for meeting the hardware requirements for the various applications becomes easier. For applications such as altimetry, where stronger signals are required, this opens up possibilities to improve the accuracy that could be achieved.

Much still needs to be done to make optimum use of the UK-DMC orbital experiment. It is planned to collect data over seas under a wide range of conditions and in the presence of independent measurements over the satellite's lifetime. Additionally, the collection of data over very rough seas (to calibrate the limits of the incoherent summation technique) and the archiving of data over land and ice surfaces will be attempted. This is all over and above the extensive analysis of the existing delay-Doppler maps that will be needed to properly understand these initial results.

This work will provide the impetus for the development of future space-based missions. Such missions should be able to provide the general public and the scientific community with measurements covering the entire globe on a timely basis. The number of available GNSS surface reflections and the low cost of this technology provide the potential to perform very dense sampling at high temporal resolution across small (mesoscale) features of the oceans surface.

The applications that this could impact are significant, ranging from global climate weather models to marine ocean safety. Eventually, the bistatically reflected signals from the GPS, and in the future Galileo constellations will develop to a point where affordable spacecraft performing ocean remote sensing using these signals can be launched on a regular basis.

ACKNOWLEDGMENT

The authors would like to thank the British National Space Centre and Surrey Satellite Technology Limited for providing the funds that made this work possible. The authors would also like to thank certain individuals for making contributions toward various aspects of this research, including D. Akos, D. Masters, and V. Zavorotny. The authors are also indebted to E. Ash, T. Allan, and all those at Satellite Observing Systems that helped to provide the QuikSCAT data used in this analysis.

The authors are greatly indebted to all those who participated in the design and realization of the experiment itself including M. Brennen, A. Woodroffe, S. Prasad, T. Plant, J. Wilhelm, N. Bean, R. Barry, the SSTL clean rooms, and European Antennas.

REFERENCES

[1] C. Cox and W. Munk, "Measurements of the roughness of the sea surface from photographs of the suns glitter," *J. Opt. Soc. Amer.*, vol. 44, pp. 838–850, Nov. 1954.

[2] M. Martin-Neira, "A Passive Reflectometry and Interferometry System (PARIS): Application to ocean altimetry," *ESA J.*, vol. 17, 1993.

[3] J. L. Garrison, S. J. Katzberg, and M. I. Hill, "Effect of sea roughness on bistatically scattered range coded signals from the global positioning system," *Geophys. Res. Lett.*, vol. 25, no. 13, pp. 2257–2260, Jul. 1, 1998.

[4] M. J. Unwin, S. Gleason, and M. Brennan, "The space GPS reflectometry experiment on the UK disaster monitoring constellation satellite," in *Proc. ION-GPS/GNSS 2003*, Portland, OR, Sep. 2003.

[5] S. Lowe *et al.*, "First spaceborne observation of an earth-reflected GPS signal," *Radio Sci.*, vol. 37, no. 1, 2002.

[6] S. Gleason *et al.*, "Preliminary attempts to connect ocean reflected GNSS signals detected from low earth orbit with sea winds and waves," presented at the *Amer. Geophysical Union Fall Meeting*, San Francisco, CA, 2004.

[7] GEC Plessey Semiconductors, *Global Positioning Products Handbook*, 1996.

[8] S. Gleason and M. J. Unwin, "Development and testing of a remote sensing instrument using GNSS reflectometry concepts," in *Proc. IGARSS*, vol. 7, Toulouse, France, 2003, pp. 4332–4334.

[9] M. Armatys, "Estimation of sea surface winds using reflected GPS signals," Ph.D. thesis, Univ. Colorado, Boulder, 2001.

[10] B. W. Parkinson, J. J. Spilker, P. Axelrad, and P. Enge, Eds., *Global Positioning System: Theory and Applications*. Washington, DC: AIAA, 1996.

[11] P. Misra and P. Enge, *Global Positioning System: Signals, Measurements, and Performance*. Lincoln, MA: Ganga-Jamuna, 2001.

[12] J. B. Tsui, *Fundamentals of Global Positioning System Receivers: A Software Approach*. New York: Wiley, 2002.

[13] M. Caparrinni, L. Ruffini, and G. Ruffini, "PARFAIT: GNSS-R coastal altimetry," presented at the *Workshop on Oceanography with GNSS-Reflections*, Jul. 2003.

[14] S. Lowe *et al.*, "State of the art GPS-reflections ocean altimetry experiment," presented at the *IGARSS*, Sydney, Australia, 2001.

[15] V. U. Zavorotny and A. G. Voronovich, "Scattering of GPS signals from the ocean with wind remote sensing application," *IEEE Trans. Geosci. Remote Sens.*, vol. 38, no. 2, pp. 951–964, Mar. 2000.

[16] T. Elfouhaily, B. Chapron, K. Katsaros, and D. Vandemark, "A unified directional spectrum for long and short wind-driven waves," *J. Geophys. Res.*, vol. 102, no. C7, pp. 15 781–15 796, Jul. 15, 1997.

[17] P. Beckmann and A. Spizzichino, *The Scattering of Electromagnetic Waves from Rough Surfaces*. Norwood, MA: Artech House, 1987.

[18] C. Elachi, *Introduction to the Physics and Techniques of Remote Sensing*, ser. John Wiley Series in Remote Sensing. New York: Wiley, 1987.

[19] S. Gleason and M. Unwin, "Ground validation of the UK disaster monitoring constellation satellite GNSS-R experiment," presented at the *GNSS Reflectometry Workshop 2003*, Barcelona, Spain, Jul. 18–19, 2003.

[20] D. E. Barrick, "Rough surface scattering based on the specular point theory," *IEEE Trans. Antennas Propogat.*, vol. AP-16, no. 4, pp. 449–454, Jul. 1968.

[21] C. Anderson, J. T. Macklin, C. P. Gommenginger, and M. A. Srokosz, "Towards a unified theoretical model of ocean backscatter for wind speed retrieval from SAR, scatterometer, and altimeter," *Can. J. Remote Sens.*, vol. 28, no. 3, pp. 354–466, 2005.

[22] J. Garrison, A. Komjathy, V. Zavorotny, and S. Katzberg, "Wind speed measurements using forward scattered GPS signals," *IEEE Trans. Geosci. Remote Sens.*, vol. 40, no. 1, pp. 50–65, Jan. 2002.

[23] A. Komjathy, V. U. Zavorotny, P. Axelrad, G. Born, and J. Garrison, "GPS signal scattering from sea surface: Comparison between experimental data and theoretical model," in *Proc. 5th Int. Conf. Marine and Coastal Environments*, San Diego, CA, 1998.

[24] F. Soulat, "Sea surface remote sensing with GNSS and sunlight reflections," Ph.D. thesis, Univ. Politecnica de Catalunya, Catalunya, Spain, Oct. 2003.

[25] G. Ruffini *et al.*, PARIS Explorer for tracking and reflectometry in L-band, Jan. 2003. Full proposal in response to the call for Earth Explorer Opportunity Missions.

[26] J. Garrison, "Anisotropy in reflected GPS measurements of ocean winds," presented at the *Workshop on Oceanography with GNSS-Reflections*, Barcelona, Spain, Jul. 2003.

[27] D. Masters, S. Katzberg, and P. Axelrad, "Airborne GPS bistatic radar soil moisture measurements during SMEX02," in *Proc. IGARSS*, vol. 2, Toulouse, France, 2003, pp. 896–898.

[28] A. Komjathy, J. Maslanik, V. Zavorotny, P. Axelrad, and S. J. Katzberg, *Sea Ice Remote Sensing Using Surface Reflected GPS Signals*. Piscataway, NJ: IEEE, 2000.

[29] T. Elfouhaily, D. R. Thompson, and L. Lindstrom, "Delay-Doppler analysis of bi-statically reflected signals from the ocean surface: Theory and application," *IEEE Trans. Geosci. Remote Sens.*, vol. 40, no. 3, pp. 560–573, Mar. 2002.
[30] D. R. Thompson, L. A. Lindstrom, R. F. Gasparovic, and T. Elfouhaily, "Doppler analysis of GPS reflections from the ocean surface," presented at the *Workshop on Oceanography with GNSS-Reflections*, Barcelona, Spain, Jul. 2003.
[31] *Radar Engineer's Handbook*, Arctec House, Norwood, MA, 1993.

Scott Gleason received the B.S. degree in electrical and computer engineering from the State University of New York, Buffalo, and the M.S. degree in engineering from Stanford University, Stanford, CA.

He has worked extensively in the space industry, having developed software for a wide range of subsystems flown on numerous spacecraft including NASA's MAP mission and the Earth Observing 1 hyperspectral imaging satellite. Since September 2001, he has been with Surrey Satellite Technology Ltd., Guildford, U.K., where his duties include GPS, AODCS, and remote sensing software development and applications research. He is presently responsible for the operation and data processing of the UK-DMC GPS experiment and is researching a Ph.D. thesis on the subject of GNSS bistatic remote sensing at the University of Surrey. His scientific interests focus on satellite remote sensing for environmental and humanitarian applications.

Stephen Hodgart received the Ph.D. degree from the University of Surrey, Guildford, U.K.

He has been with the Surrey Space Centre, Guildford, U.K., since its inception and the launch of their first satellite, UoSAT-1 in 1981. He is currently a Reader at the University of Surrey. He was responsible for the first practical low-cost active magnetic and passive gravity gradient control attitude system for a low earth orbiting satellite. He has developed novel error-correcting codes, modulation schemes, and signal processing techniques for application on low earth orbiting satellites. He was responsible for the attitude control of all the SSTL satellites that were launched from 1981 up to 1995.

Yiping Sun received the B.S. degree (with honors) from Hefei University of Technology, Hefei, China, in 1988, the M.S. degree from Beijing Institute of Technology, Beijing, China, in 1991, and the Ph.D. degree from the University of Surrey, Guildford, U.K., in 2001, all in electronics engineering.

From 1991 to 1997, he was a Senior Engineer with the Beijing Institute of Radio Measurement, working on signal processing and system study of inverse synthetic aperture radar (ISAR) and spaceborne SAR. From 2001 to 2003, he was a Principle Engineer with Lucent Technologies, Bell Laboratories, Swindon, U.K., working on the physical layer algorithms for UMTS. From January 2004 to August 2004, he was with Surrey Space Center, University of Surrey as a Research Fellow, and studying spaceborne GPS reflectometry. Now he is a Senior Researcher, with Fujitsu Laboratories of Europe, Ltd., Hayes, U.K., working on a European mobile telecommunication research project "WINNER" or 4G.

Christine Gommenginger received the Maitrise de Sciences et Techniques de la Mer from the University de Toulon et du Var, La Garde, France, the D.E.A in Electromagnetics, Telecoms, and Remote-Sensing from the University of Nice-Sophia Antipolis, France, and the Ph.D. degree from Southampton University, Southampton, U.K., on the application of low grazing angle marine radar images for dynamic ocean feature monitoring.

Her scientific interests focus on the interactions between microwave radiation and the sea surface, and the development of new microwave remote sensing techniques for oceanography and climate studies. Previous areas of research included low grazing angle microwave scattering for oil detection and wave measurements, SAR backscatter modulation by bathymetry in the coastal zone, sea state effects on altimeter wind, wave, and sea level measurements and passive microwaves for ocean salinity retrieval. She is currently with the Ocean Circulation and Climate Division, National Oceanography Centre (NOC), Southampton, U.K., and is a member of the NOC Laboratory for Satellite Oceanography.

Stephen Mackin received the B.Sc. degree in mining geology and mineral exploration from the University of Leicester, Leicester, U.K., and the Ph.D. degree from the University of Durham, Durham, U.K. His Ph.D. was based on analysis of imaging spectrometer data.

He is currently a Senior Lecturer in Remote Sensing in the Surrey Space Centre, which is part of the School of Electronics and Physical Science, University of Surrey, Guildford, U.K. He is particularly interested in applications of remote sensing and the development of a calibration and validation methodologies to be applied to a developing range of lightweight sensors for microsatellite systems.

Mounir Adjrad received the state engineering degree in electronics in 1999 and the M.Sc. degree in signal processing and communication in 2002, both from the National Polytechnic School of Algiers, Algiers, Algeria.

He was a Research Officer with the National Centre of Space Techniques of Arzew, Oran, Algeria, from 2002 to 2004. He is currently with the Surrey Space Centre, University of Surrey, Guildford, as a Research Assistant. His research interests are in the areas of statistical signal processing including array processing, performance analysis, adaptive algorithms, and applied signal processing to GPS applications.

Martin Unwin received the B.Sc. degree from Lancaster University, Lancaster, U.K., and the Ph.D. degree from the University of Surrey, Guildford, U.K.

He currently heads the GPS team at Surrey Satellite Technology, Ltd. (SSTL), responsible for spaceborne GPS receiver design and operation. He has been responsible for the GPS experiments on SSTL's satellites from PoSAT-1 in 1993, and led the design of the SGR space receiver, which has since been supplied to ESA, NASA, USAF, and an International Space Station application. Prior to working at SSTL, he was involved in microwave tube design at Thorn Microwave Devices Ltd.